Dependence of Tyrosine Oxidation in Highly Oxidizing Bacterial Reaction Centers on pH and Free-Energy Difference†

L. Kálmán,‡,§ A. J. Narváez,‡,|| R. LoBrutto,⊥ J. C. Williams,‡ and J. P. Allen*,‡

Department of Chemistry and Biochemistry and School of Life Sciences, Arizona State University, Tempe, Arizona 85287-1604

Received December 17, 2003; Revised Manuscript Received August 5, 2004

ABSTRACT: The pH and temperature dependences of tyrosine oxidation were measured in reaction centers from mutants of *Rhodobacter sphaeroides* containing a tyrosine residue near a highly oxidizing bacteriochlorophyll dimer. Under continuous illumination, a rapid increase in the absorption change at 420 nm was observed because of the formation of a charge-separated state involving the oxidized dimer and reduced primary quinone, followed by a slow absorption decrease attributed to tyrosine oxidation. Both the amplitude and rate of the slow absorption change showed a pH dependency, indicating that, at low pH, the rate of tyrosine oxidation is limited by the transfer of the phenolic proton to a nearby base. Below 17 °C, the rate of the slow absorption change had a strong exponential dependence on the temperature, indicating a high activation energy. At higher pH and temperature, the overall rate of tyrosyl formation appears to be limited by a proposed conformational change in the reaction center that is also observed in reaction centers that do not undergo tyrosine oxidation. The yield of tyrosyl formation measured using electron paramagnetic resonance spectroscopy decreased significantly at 4 °C compared to 20 °C and was lower at both temperatures in mutants expected to have a slightly smaller driving force for tyrosyl formation.

The primary process of photosynthesis, the conversion of light energy into chemical energy, is performed by pigment−protein complexes termed reaction centers in purple photosynthetic bacteria and photosystems I and II in plants, algae, and cyanobacteria (*1*, *2*). The reaction center and photosystem II are evolutionarily related and share structural similarity in that the core cofactors and subunits are symmetrically arranged into two branches (*3*−*5*). Excitation of the bacteriochlorophyll dimer, P,[1] in bacterial reaction centers, or the primary electron donor of photosystem II, P_{680}, results in a unidirectional transmembrane electron transfer to the primary and secondary quinones, through one of the two branches of cofactors. Despite these structural and functional similarities, P_{680} of photosystem II has the unique ability to catalyze the oxidation of water into molecular oxygen. The oxidization of water in photosystem II is achieved by three factors: the high oxidizing potential of P_{680}, the ability of a key tyrosine residue, Y_Z, to couple the transfer of electrons and protons, and the presence of a manganese cluster that can store the four electron equivalents required for the overall reaction. Some of these attributes, such as a highly oxidizing P, coupling of electron and proton transfer through a tyrosine residue, and oxidation of manganese, can be introduced into bacterial reaction centers by genetic manipulation (*6*, *7*).

In biological systems, tyrosyl formation has been shown to be coupled to the transfer of the phenolic proton to a nearby base (*8*). Because the formation of protonated tyrosyl radicals is energetically unfavorable, the transfer of the phenolic proton either precedes electron transfer or occurs in a concerted manner with electron transfer. In both cases, the rate of tyrosyl radical formation is dependent upon the rate of both electron and proton transfers. For the bacterial reaction center, the situation is complicated by the low yield of tyrosyl radical formation, requiring the use of continuous illumination to increase the amount of the tyrosyl radical. Earlier reports have shown that, when the charge-separated state involving the oxidized dimer and the reduced primary quinone ($P^+Q_A^-$) is produced by continuous illumination, the lifetime of this state can increase up to 7000-fold with respect to the lifetime of the flash-induced charge-separated state (*9*−*11*). This dramatic effect was interpreted as arising from conformational changes caused by prolonged continuous illumination. Light-induced conformational changes associated with the secondary quinone have also been reported in several other experiments, including X-ray diffraction studies (*12*−*16*). Therefore, there may be a relationship between tyrosyl formation and conformational changes arising from prolonged exposure to light.

Several mutations incorporated into reaction centers have been used to manipulate the P/P^+ midpoint potential and to introduce tyrosine residues near the dimer (Table 1). To achieve a highly oxidizing potential in reaction centers, three hydrogen bonds were introduced to P by the mutations Leu to His at L131, Leu to His at M160, and Phe to His at M197

† This work was supported by Grant MCB 0131764 from the NSF.

* To whom correspondence should be addressed. Phone: (1)-480-965-8241. Fax: (1)-480-965-2747. E-mail: jallen@asu.edu.

‡ Department of Chemistry and Biochemistry.

§ Permanent address: Department of Biophysics, University of Szeged, Egyetem u.2, H-6722, Szeged, Hungary.

|| Present address: Department of Biochemistry and Biophysics, Stockholm University, Sweden.

⊥ School of Life Sciences.

[1] Abbreviations: P, bacteriochlorophyll dimer; Q_A, primary quinone; EPR, electron paramagnetic resonance.

10.1021/bi0362727 CCC: $27.50
Published on Web 09/21/2004

Table 1: Mutants of *Rhodobacter sphaeroides*

name	$\delta\Delta G°$ [a] (mV)	mutations[b]								
quadruple		LH(L131)	+	LH(M160)	+	FH(M197)	+	YW(M210)		
Y_L		LH(L131)	+	LH(M160)	+	FH(M197)	+	YW(M210)	+	RY(L135)
Y_M	0	LH(L131)	+	LH(M160)	+	FH(M197)	+	YW(M210)	+	RY(M164)
Y_M'	−60	LH(L131)			+	FH(M197)	+	YW(M210)	+	RY(M164)
Y_M''	−85			LH(M160)	+	FH(M197)	+	YW(M210)	+	RY(M164)

[a] $\delta\Delta G°$ is the change in the free-energy difference for tyrosine formation in the mutants compared to the Y_M mutant, assuming that this difference is directly related to the expected change of the P/P^+ midpoint potential. [b] Mutations are written with the first letter representing the amino acid in the wild type, the second letter representing the residue in the mutant, and the position denoted in the parenthesis; for example, LH(L131) is the Leu to His mutation at amino acid residue L131.

(*17*). Each of these mutations raises the midpoint potential by a consistent amount when combined with other mutations, and a triple mutant containing all three was found to have a P/P^+ midpoint potential of 0.76 V compared to a potential of 0.5 V for wild-type reaction centers. The triple mutant is still capable of transferring an electron from P to Q_A and then to the secondary quinone, but the quantum yield is decreased because of a decrease in the free-energy difference for the initial charge-separated state (*18*). The quadruple mutant has an additional mutation of Tyr to Trp at M210, resulting in the P/P^+ midpoint potential being further elevated to above 0.8 V (*6*). When tyrosine residues were introduced at L135 and M164 in reaction centers with these four mutations, producing the Y_L and Y_M mutants, respectively, the introduced tyrosines were found to serve as secondary electron donors, resulting in the formation of a tyrosyl radical after exposure to light (*6*, *19*, *20*). Two additional mutants, Y_M' and Y_M'', do not have the leucine to histidine mutations at M160 and L131, respectively, found in the Y_M mutant. The removal of these mutations should result in P/P^+ midpoint potentials that are lower by 60 and 85 mV, respectively, compared to the Y_M mutant and in commensurate decreases in the free-energy difference for tyrosine oxidation. In this study, we investigate tyrosyl formation in these mutants by monitoring the light-induced changes in the optical spectra as the pH and temperature were varied. The relative yield of tyrosyl formation was determined using electron paramagnetic resonance (EPR) spectroscopy at different temperatures.

MATERIALS AND METHODS

Construction of Mutants, Protein Isolation, and Sample Preparation. The construction of the quadruple, Y_L, and Y_M mutants has been described previously (*6*). The Y_M' and Y_M'' mutants were constructed from *Rhodobacter sphaeroides* using methods described previously (*17*). Cells were grown semiaerobically, and the reaction centers were prepared as described earlier, except that Triton X-100 was used for the ion-exchange chromatography step instead of lauryl dimethylamine oxide (*21*). The assay solution contained 0.03% Triton X-100, 1 mM EDTA, 100 mM NaCl, and 15 mM Mes (2-(*N*-morpholino)ethanesulfonic acid), Hepes (*N*-[2-hydroxyethyl]piperazine-*N*′-[2-ethane]sulfonic acid), Tris (tris(hydroxymethyl)aminomethane), or CHES (2-[*N*-cyclohexylamino]ethane sulfonic acid), depending on the pH. Measurements were performed in the presence of 100 μM terbutryne to block electron transfer to the secondary quinone unless stated otherwise.

Measurement of Absorption Changes. A Cary 5 spectrophotometer (Varian) was used to measure the optical absorption changes induced by continuous light illumination. Because of the extensive photodegradation of the reaction centers upon prolonged and high-intensity illumination, nonsaturating, short, continuous illumination was used from an Oriel tungsten lamp with an 860 nm interference filter. At room temperature, the illumination lasted no longer than 30 s, and the intensity was reduced to about one-third of the saturating value of the wild type. At lower temperatures, the protein degradation because of prolonged illumination was less pronounced, and therefore the illumination time was extended up to 45 s. The spectra were recorded using a fast scanning rate of 900 nm/min. Flash-induced absorption transients were measured at 865 nm by a single beam spectrophotometer of local design (*22*). The reaction centers were excited at 532 nm with a 5 ns laser pulse using a ND:YAG laser (Continuum), and the kinetic traces were analyzed using exponential decomposition.

EPR Spectroscopy. The EPR measurements were performed using a Bruker E580 X-band spectrometer with a magnetic field modulation frequency of 100 kHz, an amplitude of 0.4 mT, a microwave power of 10 mW, and a microwave frequency of approximately 9.64 GHz. Reaction centers were concentrated for the EPR measurements in a Centricon microconcentrator (Amicon) up to 300 μM. Samples were placed in a quartz standard EPR tube, illuminated at 4 or 20 °C, and the radicals were trapped by immersing the sample tubes into an ethanol/dry ice bath. The spectra were obtained at 125 K by averaging several scans. Determination of the relative radical populations in the EPR spectra was performed by fitting the spectra to a linear combination of the spectrum of the P^+ radical, represented by the spectrum from the wild type, and the spectrum of the tyrosyl radical, as represented by the spectrum of the Y_M mutant at pH 10.2 (*23*).

RESULTS

Light-Induced Conformational Changes. For the quadruple and the Y_L mutants, light-induced changes in the optical spectra were measured in the 400−500 nm region (Figure 1). The spectrum of the quadruple mutant features a broad positive band that is centered at 430 nm arising from the $P^+Q_A^-$ state. In the presence of the spectrally silent electron donor, diamino durene (DAD), P^+ is rapidly reduced and the spectrum has a positive band at 450 nm that is characteristic of anionic semiquinones. For the Y_L mutant, the spectrum shows the same positive band at 450 nm indicating the presence of the state PQ_A^- with the additional features of an absorption decrease at 420 nm and an increase around 407 nm that were not present in the spectrum of the quadruple mutant. Spectra measured for the Y_M mutant (data

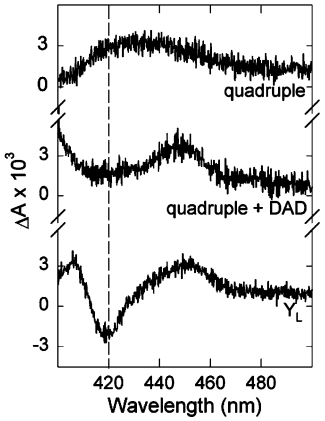

FIGURE 1: Light-minus-dark difference optical spectra of the quadruple and Y_L mutants at pH 9.0 in the 400−500 nm spectral region. The absorption changes at 420 nm (vertical dashed line) are in the opposite direction in the quadruple and the Y_L mutants, indicating the presence of different redox states. In the quadruple mutant, the broad positive band around 430 nm is characteristic of the $P^+Q_A^-$ state (upper trace). In the presence of the spectrally silent secondary electron donor DAD, the features of P^+ are no longer detectable. The band at 450 nm represents the Q_A^-/Q_A difference spectrum (middle trace). In the Y_L mutant, Tyr L135 donates an electron to P^+, revealing the spectral features of the tyrosyl radical at 420 and 407 nm together with those of Q_A^- at 450 nm. Conditions: 1.5 μM reaction center in 0.03% Triton X-100, 15 mM Ches at pH 9.0, 1 mM EDTA, 100 mM NaCl, and 100 μM terbutryne.

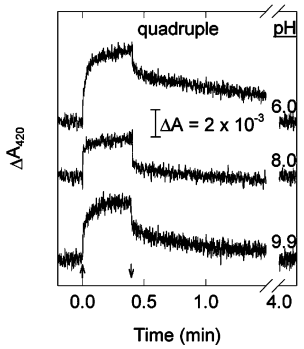

FIGURE 2: Kinetic traces of the light-induced absorption changes at 420 nm measured in the quadruple mutant at different pH values. The arrows show the time when the light was turned on and off. Two kinetic phases can be distinguished during illumination. The fast absorption change, which is not resolved, is assigned to formation of the $P^+Q_A^-$ state from the dark-adapted conformation. The slow absorption change during the illumination is associated with reaction centers in a different, light-adapted conformation. Conditions are the same as indicated in the Figure 1 caption, except that Mes, Hepes, Tris, or Ches was used as the buffer, depending on the pH.

not shown) were similar to that of the Y_L mutant. The spectral features at 407 and 420 nm have been identified as indicators of the presence of a $Y^{\cdot}PQ_A^-$ state (*6*, *19*, *24*).

For the quadruple mutant, the kinetics of the light-induced absorption changes at 420 nm upon a short illumination were measured at different pH values (Figure 2). Upon exposure to light, the absorption at 420 nm increased because of the formation of the $P^+Q_A^-$ state, and this signal fully recovered in the dark. The initial absorption increase was too fast to be resolved using the spectrophotometer. This initial rise was followed by a slower increase during the illumination. After the illumination was stopped, the absorption increase decayed fully in a biphasic manner. A similar kinetic profile was

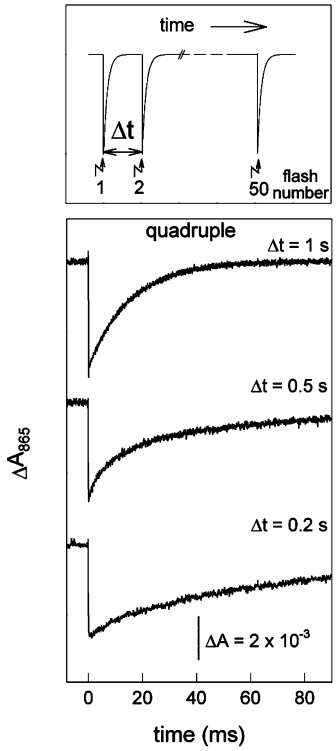

FIGURE 3: Dependence of the kinetics of the flash-induced $P^+Q_A^- \rightarrow PQ_A$ charge recombination on the delay time (Δt) between the flashes in reaction centers from the quadruple mutant at pH 9. Upper panel shows the algorithm by which the traces in the lower panel were collected. A total of 50 traces were averaged, and Δt was varied from 1 to 0.2 s. At 1 s delay time, the charge recombination was monophasic with a 15 ms lifetime. As the delay time was decreased to 0.5 and 0.2 s, the charge recombination became biphasic and another much slower component with an approximately 60 ms lifetime was accumulated during the averaging of the traces. Conditions of the assay solution were the same as indicated in the Figure 1 caption.

recorded at 865 nm, where only P^+ contributes (data not shown).

The measurements were performed in the presence of terbutryne, which blocks transfer to the secondary quinone; therefore, the $P^+Q_A^-$ state was rapidly formed because of the illumination. The slow increase in absorption at 420 nm during illumination arises from a slow increase in the total amount of reaction centers in a charge-separated state after the fast, initial formation. The two kinetic phases should represent two different populations of the reaction centers that are both in the $P^+Q_A^-$ state. The two populations can be attributed to the reaction centers having two conformations with significantly different lifetimes. The same kinetics of a rapid absorption increase followed by a slow absorption increase is observed at 865 nm in both the quadruple mutant and wild-type reaction centers. In the wild type, the slow increase at 865 nm has previously been attributed to the presence of a light-induced conformational change that results in a long-lived $P^+Q_A^-$ state (*9*−*11*). Thus, our results for the quadruple mutant indicate that such a long-lived state is also formed in the quadruple mutant.

To confirm the presence of a long-lived component in the kinetics, the response of the quadruple mutant to a series of light pulses was measured with different delay times between pulses (Figure 3). After a single flash, the $P^+Q_A^- \rightarrow PQ_A$ charge recombination process occurs with a 15 ms time

constant compared to 100 ms for the wild type, consistent with the increase in the P/P^+ midpoint potential (*6*, *17*). An exponential decrease in the absorption change that is completed within 50 ms after the flash is seen in the averaged trace with a 1 s delay between the flashes. As the delay between the flashes was made shorter to 0.5 and 0.2 s, the kinetics of the charge recombination became biphasic.

This altered behavior can be understood with the assumption that there are at least two different states of the reaction center. One is the dark-adapted state that has a 15 ms lifetime, and the second is a long-lived, conformationally changed state. As has been previously proposed for the wild type (*9*−*11*), the long-lived conformationally changed state is generated from the charge-separated state. Upon illumination of dark-adapted reaction centers by a single flash, the $P^+Q_A^-$ state is formed. Competing with the decay of the short-lived $P^+Q_A^-$ state is the slow formation of a conformationally changed $P^+Q_A^-$ state. Once formed, the conformationally changed $P^+Q_A^-$ state first decays to a conformationally changed neutral PQ_A state and subsequently decays to the original dark-adapted PQ_A state. When the time between flashes is long, the charge recombination reactions have time to fully occur and the small fraction of the reaction centers that underwent the conformational change has time to recover to the dark-adapted state. Thus, the reaction centers will be all in the dark-adapted state upon illumination by the second flash, and the recovery after the second flash will match the original kinetics. When the time between flashes is decreased, the conformationally changed reaction centers have time to recover to a neutral state but do not have time to recover to the original dark-adapted state. Thus, the second flash will illuminate both the dark-adapted reaction centers and a small fraction of neutral conformationally altered reaction centers, which will form the conformationally altered $P^+Q_A^-$ state. This situation generates heterogeneity in the population of the reaction centers and in the charge recombination kinetics. As the time between the flashes becomes shorter, more of the conformationally altered reaction centers are observed. Similarly, the use of continuous illumination in these experiments would drive a significant part of the reaction centers into the longer-lived, conformationally changed $P^+Q_A^-$ state. The kinetics of the decays shown are highly dependent upon the time between the flashes, and so the lifetime of the light-adapted states cannot be determined from these traces but must be measured using steady-state illumination conditions, as has been discussed elsewhere (*9*−*11*).

Kinetics of Tyrosyl Radical Formation. In general, during illumination of the Y_L mutant, an initial absorption increase at 420 nm was followed by a slow absorption decrease (Figure 4). After the light was switched off, a rapid absorption decrease was followed by a slow recovery. The sharp absorption increase at the beginning of the illumination arises from formation of the $P^+Q_A^-$ state from the dark-adapted conformation. While under illumination, the reaction centers can undergo a conversion to the long-lived conformationally changed $P^+Q_A^-$ state, and accumulation of this state would result in a slow increase in the absorption at 420 nm. The reaction centers can also form the $Y^{\cdot}Q_A^-$ state, leading to a decrease in the absorption at 420 nm. The slow absorption decrease under illumination can be assigned to formation of the $Y^{\cdot}Q_A^-$ state, presumably by tyrosine

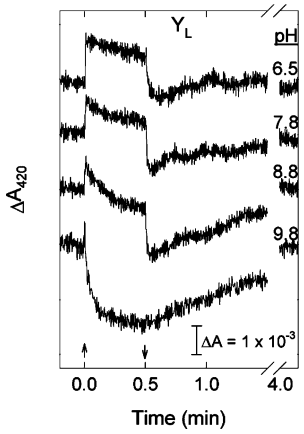

FIGURE 4: Representative kinetic traces of the light-induced absorption changes at 420 nm measured in the Y_L mutant at different pH values at room temperature. The arrows show the time when the light was turned on and off. Conditions are the same as indicated in the Figure 2 caption.

oxidation from the long-lived $P^+Q_A^-$ state. Measurement at 865 nm under similar conditions shows absorption changes that indicate a slow decrease in the total amount of P^+ during illumination (data not shown), consistent with this assignment of the slow absorption decrease at 420 nm under illumination as being associated with tyrosyl formation. Comparable kinetics seen in proton release and electron paramagnetic resonance measurements (*6*, *7*, *20*) also confirm a slow accumulation of $Y^{\cdot}$ during illumination. The sharp decrease after illumination is due to charge recombination from the dark-adapted $P^+Q_A^-$ state as has been measured at 865 nm using a single laser flash (data not shown). The subsequent slow absorption change in the dark is associated with recovery from both the conformationally changed $P^+Q_A^-$ state and the $Y^{\cdot}Q_A^-$ state.

Based upon previous studies (*6*, *19*, *24*), the $P^+Q_A^-$ state is favored over the $Y^{\cdot}Q_A^-$ state at low pH. For example, at pH 6.5, the extent of the slow absorption decrease during illumination that is attributed to the $Y^{\cdot}Q_A^-$ state is small compared to the absorption increase because of the $P^+Q_A^-$ state. Upon increasing the pH, the extent of the slow absorption decrease becomes larger, reflecting an increasing contribution of the $Y^{\cdot}Q_A^-$ state. At pH 9.8, P^+ is mostly reduced by Tyr L135, so that at the end of the illumination the $Y^{\cdot}Q_A^-$ state dominates, and there is no measurable $P^+Q_A^-$ state, indicated by the lack of a sudden decrease as the light is switched off. The rate of the slow absorption decrease during illumination was observed to become faster with increasing pH. The Y_M mutant shows similar behavior to the Y_L mutant, although the pH dependence is shifted.

The strong dependence on pH of the amplitude of the slow component of the absorption change under illumination at 420 nm in the quadruple, Y_L, and Y_M mutants showed systematic patterns (Figure 5A). For the quadruple mutant, the amplitude of the slow phase was always positive with a minimal value near pH 8. This pH dependence profile of the slow component is similar to that measured at 865 nm in the carotenoid-less R-26 strain (*10*). For the Y_L and Y_M mutants, the amplitude of the slow phase was always negative and became more negative with increasing pH. The amplitude of the slow phase could be characterized with single Henderson−Hasselbalch-type curves, with pK_a values of 6.8

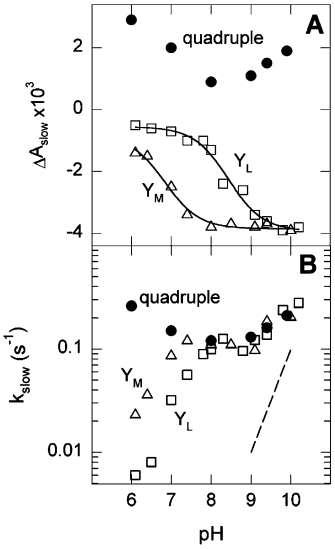

FIGURE 5: Amplitude change at 420 nm, ΔA_{slow}, and rate of formation, k_{slow}, of the slow kinetic component measured at different pH values in the Y_L (□), Y_M (△), and quadruple (●) mutants. (A) Amplitude change is the change in absorption at 420 nm during the illumination time after the initial rise because of the fast component. The solid curves are Henderson−Hasselbalch-type fits using single protonatable residues with pK_a values of 6.83 ± 0.12 and 8.43 ± 0.10 for the Y_M and Y_L mutants, respectively. (B) Rate of formation of the slow kinetic component was determined from a single-exponential fit of the change in absorbance at 420 nm during illumination after the initial rise. The dashed line represents a slope of 1 order of magnitude change in rate over 1 pH unit. Conditions are the same as indicated in the Figure 2 caption.

and 8.4 for the Y_M and Y_L mutants, respectively. These pK_a values are similar to those obtained from previous determinations of light-induced changes of the optical spectra associated with tyrosyl formation (*6*, *19*).

The pH dependence of the rate of formation of the slow phase also showed distinct features (Figure 5B). For the quadruple mutant, the pH dependence of the rate was weak with values of 2.6×10^{-1} and 2.1×10^{-1} s^{-1} at pH 6 and 10, respectively, and a minimal value of 1.2×10^{-1} s^{-1} near pH 8. In contrast, for both the Y_L and Y_M mutants, increasing the pH resulted in a sharp increase in the rate, up to a pH corresponding to the pK_a determined from the fit of the pH dependence of the amplitude. For lower pH values, the slope of the increase was close to 1 order of magnitude over 1 pH unit, suggesting the involvement of a proton in the reaction. At pH values above the pK_a, the measured rates in the Y_L and Y_M mutants were essentially identical to the rate measured for the quadruple mutant.

The temperature dependence of the formation rate of the slow component of the light-induced absorption changes at 420 nm was determined in the mutants at pH 9.0 between 4 and 30 °C (Figure 6). For the quadruple mutant, the rate decreased as the temperature decreased, following an exponential dependence, suggesting an Arrhenius relationship with an activation energy of 37 ± 4 kJ/mol. The Y_L and Y_M mutants showed a behavior that was similar to each other and that was more complex than observed for the quadruple mutant. Below 17 °C, the rate was much more strongly dependent upon temperature than in the quadruple mutant. A fit of the combined data from both the Y_L and Y_M mutants using an Arrhenius-type dependence yielded an activation energy of 125 ± 10 kJ/mol. Above 17 °C, the Y_L and Y_M

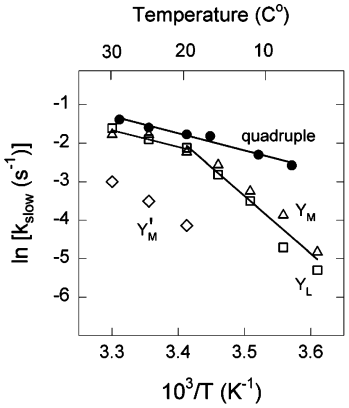

FIGURE 6: Temperature dependence of the formation of the slow kinetic component during illumination in reaction centers of the quadruple (●), Y_L (□), Y_M (△), and Y_M' (◇) mutants at pH 9.0. The dependence below 17 °C was much steeper than above 17 °C, with the slopes of Arrhenius plots yielding activation energies of 125 ± 10 and 36 ± 5 kJ/mol, respectively, for the combined data for the Y_L and Y_M mutants. For the quadruple mutant, the fit yielded an activation energy of 37 ± 4 kJ/mol that presumably is associated with the proposed conformational change of the $P^+Q_A^-$ state. Conditions are the same as indicated in the Figure 1 caption.

mutants had a much weaker dependence on the temperature, with an activation energy of 36 ± 5 kJ/mol. This dependence matched that of the quadruple mutant.

The rate of formation of the slow component was measured in the Y_M' mutant at pH 9. The amplitude was small compared to the Y_M and Y_L mutants, and the temperature dependence could only be measured above 20 °C because at lower temperatures during the illumination no slow absorption decrease at 420 nm was observed in the optical kinetic traces. In this mutant, the rate was significantly slower than that of the Y_M and Y_L mutants, with rates of 1.6×10^{-2} to 5.0×10^{-2} s^{-1} from 20 to 30 °C, compared to rates of 1.5×10^{-1} to 2.0×10^{-1} s^{-1} for both of the other two mutants in this same temperature region (Figure 6).

Yield of Tyrosyl Radical Formation. The relative amplitudes of the $Y^{\cdot}$ and P^+ species were determined in light-minus-dark EPR spectra of the Y_M, Y_M', and Y_M'' mutants at 4 and 20 °C at pH 9. At the lower temperature in the Y_M mutant, the spectra shifted to lower *g* values (data not shown), compared to spectra that have been assigned to a tyrosyl radical and are observed at higher temperatures (*6*, *19*), indicating the retardation of the tyrosyl radical formation at lower temperatures with a resulting increase in the relative amount of P^+. The ratio of $Y^{\cdot}/P^+$ was similar for the three mutants at 4 °C, with values ranging from 0.78 to 1.0 (Figure 7). The measurements at 20 °C showed pronounced differences among the mutants with values for the $Y^{\cdot}/P^+$ ratio of 0.89, 1.32, and 4.26 for the Y_M'', Y_M', and Y_M mutants, respectively.

DISCUSSION

Bacterial reaction centers with highly oxidizing bacteriochlorophyll dimers are able to specifically oxidize nearby tyrosine residues (*6*). Tyrosine oxidation in this bacterial system is sensitive to pH and to the identity of the proton-accepting base (*6*, *19*). The phenolic proton is either released to the bulk or retained within the protein, depending upon the position of the introduced tyrosine (*20*, *24*). In this work, the rate of formation of tyrosyl radicals in bacterial reaction

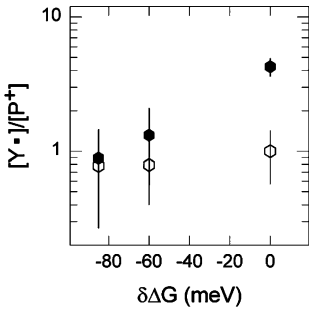

FIGURE 7: Dependence of the ratio of $Y^{\cdot}/P^{+}$ in EPR spectra on the changes in the free-energy difference for tyrosyl formation at 4 (⬡) and 20 °C (⬢). The changes in the free-energy difference are assumed to be equal to the estimated changes in the P/P^{+} midpoint potentials of the Y_M'' and Y_M' mutants compared to the Y_M mutant (Table 1). The data points represent the average of several independent measurements, and the individual error bars are shown.

centers was found to be sensitive to pH, temperature, and the midpoint potential of the dimer.

Because of the relatively slow rate of formation, continuous light is used to observe tyrosyl radical formation in bacterial reaction centers. After single flash excitation, the stable $P^{+}Q_A^{-}$ charge pair undergoes charge recombination with a lifetime of 14−17 ms, depending on the mutant and pH (Figure 3). Decreasing the time between the flashes or the use of continuous illumination (Figure 2) makes the recovery kinetics of the oxidized dimer biphasic. The altered behavior arises from the formation of a long-lived form of the $P^{+}Q_A^{-}$ state, probably representing a conformationally altered state. At room temperature and at pH values higher than the pK_a of the proton acceptor base, the rate of tyrosine oxidation for the Y_M and Y_L mutants is the same as the rate of the proposed conformational change (Figure 5). This observation strongly suggests that the limiting precursor reaction in the tyrosine oxidation is the light-induced conformational rearrangement of the reaction-center protein. In the wild type or carotenoid-less R-26 strain, the lifetime of the charge-separated state can increase up to 7000-fold, depending upon the illumination conditions (*9*−*11*). These earlier reports suggested that during continuous illumination, the local environment of P^{+} or Q_A^{-} changes, resulting in a substantially longer lifetime of the oxidized dimer compared to its lifetime in the dark-adapted conformation. The actual effect of such a conformational change on tyrosine oxidation in the mutants is not known, but the conformational change appears to be a necessary precursor to tyrosine oxidation.

For tyrosine oxidation, once the reaction centers have been poised in the putative conformationally altered state by the use of continuous illumination, both a proton and an electron transfer must occur to produce a stable neutral tyrosyl radical. At low pH values, the protonated base near the tyrosine presumably retards the proton transfer, consistent with the slower overall rate of tyrosyl formation in the Y_M and Y_L mutants compared to the rate of the conformational change seen in the quadruple mutant (Figure 5). However, at pH values above the associated pK_a, the deprotonated base can accept the phenolic proton. This electron−proton coupled reaction can proceed by several different possible pathways (*25*, *26*). One possibility is for electron transfer to precede proton transfer. However, this would require the transient formation of a protonated tyrosyl radical, which is energetically extremely unfavorable at room temperature (*27*, *28*). Therefore, the most likely pathway involves initially the transfer of the phenolic proton to a nearby base, followed by the transfer of the electron from the tyrosine to P^{+}. For this process, after transfer to the closest or primary proton acceptor of the phenolic proton, there may be subsequent transfer steps involving a set of protonatable residues transferring the proton away from the tyrosinate.

The observed rate constant k_{slow}, the rate of the slow component of the absorption changes under illumination, decreased with decreasing temperature (Figure 6). For the quadruple mutant, the rate constant k_{slow} was only weakly dependent upon temperature and the activation energy was small and presumably associated with the conformational change. For the Y_L and Y_M mutants, the temperature dependence of k_{slow} was more pronounced at low temperatures than at room temperature. At 4 °C, the dependence of the rate upon temperature suggests that proton transfer or the conformational change is rate-limiting because of the large activation energy of 125 kJ/mol. The larger activation energy indicates an unfavorable protonation equilibrium, which might involve elongation of the distance between the tyrosine and the proton acceptor or disruption in the proton-conducting network of protonatable residues as the protein is cooled. An alternative explanation for the larger activation energy in the Y_L and Y_M mutants compared to the quadruple mutant is that the conformational change in the Y_L and Y_M mutants is different than in the quadruple mutant. However, the conformational change is associated with P^{+}, and the amino acid environment and spectral properties of P are unchanged in the three mutants. Thus, the activation energy associated with the conformational change should be the same for these mutants, and the most likely interpretation is that the differences in the activation energies arise because of the proton-transfer associated with the tyrosine oxidation process in the Y_L and Y_M mutants.

The measured dependence of the ratio of $Y^{\cdot}/P^{+}$ on the change in the free-energy difference in the mutants was strikingly different at 4 and 20 °C (Figure 7). Neither set of data showed the dependence on the free-energy difference expected for a true equilibrium. Interpretation of the observed dependence is complicated because the concentrations are determined under steady-state illumination conditions and the populations reflect the combination of several forward and reverse reactions. At 20 °C, an activated electron-transfer process may limit the formation of the tyrosyl radical in the mutants with a small free-energy difference. At 4 °C, the ratio is independent of the free-energy difference, suggesting that the formation of the tyrosyl radical is limited by a different reaction, such as proton transfer, which is not expected to depend on the free-energy difference, rather than on an electron-transfer reaction. Any interpretation must also assume that the calculated changes in free-energy difference are the correct values and that they do not change with temperature.

Although rates of tyrosine oxidation in photosystem II, 10^2 and 10^7 s^{-1} for Y_D and Y_Z, respectively (*29*), are faster than the rates reported for the Y_L and Y_M mutants, the relative order of the electron and proton transfers is probably similar. Formation of the tyrosyl radical in Mn-depleted photosystem II has been modeled as arising from intermediate formation of a tyrosinate by proton transfer followed by electron

transfer (*26*). For artificial systems, the process of oxidation of tyrosine by ruthenium has been modeled as arising from a concerted process (*30*). In both of these other systems, the observed rates are several orders of magnitude faster than those reported here, presumably because of the rate-limiting step of the conformational change in the reaction center, which must precede tyrosine oxidation in these mutants. The pH-dependent pattern of the rates of tyrosyl radical formation determined in this study is remarkably similar to that measured in photosystem II or related artificial systems (*30*, *31*). In all systems, including this one, the observed rates of tyrosine oxidation at room temperature increase steeply up to approximately the pK_a of the putative proton acceptors. The slope of this increase was close to 1 order of magnitude per 1 pH unit in both the Y_M and Y_L mutants. The value of the slope suggests the necessity of the removal of the phenolic proton upon the reaction. Once the light-adapted conformation is formed, at low pH, the tyrosine oxidation reaction is limited by the proton transfer, while at higher pH values only the conformational change is the rate-determining step.

In conclusion, the formation of the tyrosyl radical in the reaction centers depended in systematic ways upon the pH, temperature, and the P/P^+ midpoint potential. The yield of tyrosyl formation increased as the pH increased from 6 to 10, demonstrating the coupling to proton transfer. The overall process of tyrosyl formation, including a precursor conformational change, exhibited a strong activation energy, consistent with a decrease in the yield of tyrosyl formation at lower temperatures for the Y_M mutant. At low temperatures, the yield was similarly limited for mutants with different driving forces. However, at higher temperatures, a distinct dependence of the yield on the driving force was observed. We speculate that this difference in the driving force dependence is due to a change in the relative rates of proton and electron transfers with temperature. One possible mechanism consistent with the data is an initial conformational change, followed by rapid proton transfer and subsequent rate-limiting electron transfer at room temperature, while at low temperatures, proton transfer is rate-limiting. The highly oxidizing reaction centers are a useful model system for studying tyrosine oxidation because certain key parameters, such the free-energy difference, can be systematically altered in the bacterial system.

REFERENCES

1. Blankenship, R. E., Madigan, M. T., and Bauer, C. E., Eds. (1995) *Anoxygenic Photosynthetic Bacteria*, Kluwer Academic Publishers, Dordrecht, The Netherlands.
2. Ort, D. R., and Yokum, C. F., Eds. (1996) *Oxygenic Photosynthesis: The Light Reactions*, Kluwer Academic Publishers, Dordrecht, The Netherlands.
3. Deisenhofer J., and Michel, H. (1989) The photosynthetic reaction center from the purple bacterium *Rhodopseudomonas viridis*, *Science 245*, 1463−1473.
4. Feher, G., Allen, J. P., Okamura, M. Y., and Rees, D. C. (1989) Structure and function of bacterial photosynthetic reaction centres, *Nature 339*, 111−116.
5. Zouni, A., Witt, H. T., Kern, J., Fromme, P., Krauss, N., Saenger, W., and Orth, P. (2001) Crystal structure of photosystem II from *Synechococcus elongatus* at 3.8 Å resolution, *Nature 409*, 739−743.
6. Kálmán, L., LoBrutto, R., Allen, J. P., and Williams, J. C (1999) Modified reaction centres oxidize tyrosine in reactions that mirror photosystem II, *Nature 402*, 696−699.
7. Kálmán, L., LoBrutto, R., Williams, J. C., and Allen, J. P. (2003) Manganese oxidation by modified reaction centers from *Rhodobacter sphaeroides*, *Biochemistry 42*, 11016−11022.
8. Tommos, C., and Babcock, G. T. (2000) Proton and hydrogen currents in photosynthetic water oxidation, *Biochim. Biophys. Acta 1458*, 199−219.
9. Goushcha, A. O., Kharkyanen, V. N., and Holzwarth, A. R. (1997) Nonlinear light-induced properties of photosynthetic reaction centers under low intensity irradiation, *J. Phys. Chem. B 101*, 259−265.
10. Kálmán, L., and Maróti, P. (1997) Conformation-activated protonation in reaction centers of the photosynthetic bacterium *Rhodobacter sphaeroides*, *Biochemistry 36*, 15269−15276.
11. van Mourik, F., Reus, M., and Holzwarth, A. R. (2001) Long-lived charge-separated states in bacterial reaction centers isolated from *Rhodobacter sphaeroides*, *Biochim. Biophys. Acta 1504*, 311−318.
12. Kleinfeld, D., Okamura, M. Y., and Feher, G. (1984) Electron-transfer kinetics in photosynthetic reaction centers cooled to cryogenic temperatures in the charge-separated state: Evidence for light-induced structural changes, *Biochemistry 23*, 5780−5786.
13. Stowell, M. H. B., McPhillips, T. M., Rees, D. C., Soltis, S. M., Abresch, E., and Feher, G. (1997) Light-induced structural changes in photosynthetic reaction center: Implications for mechanism of electron−proton transfer, *Science 276*, 812−816.
14. McMahon, B. H., Müller, J. D., Wraight, C. A., and Nienhaus, G. U. (1998) Electron transfer and protein dynamics in the photosynthetic reaction center, *Biophys. J. 74*, 2567−2587.
15. Xu, Q., and Gunner, M. R. (2001) Trapping conformational intermediate states in the reaction center protein from photosynthetic bacteria, *Biochemistry 40*, 3232−3241.
16. Fritzsch, G., Koepke, J., Diem, R., Kuglstatter, A., and Baciou, L. (2002) Charge separation induces conformational changes in the photosynthetic reaction centre of purple bacteria, *Acta Crystallogr., Sect. D 58*, 1660−1663.
17. Lin, X., Murchison, H. A., Nagarajan, V., Parson, W. W., Allen, J. P., and Williams, J. C. (1994) Specific alteration of the oxidation potential of the electron donor in reaction centers from *Rhodobacter sphaeroides*, *Proc. Natl. Acad. Sci. U.S.A. 91*, 10265−10269.
18. Allen, J. P., and Williams, J. C. (1995) Relationship between the oxidation potential of the bacteriochlorophyll dimer and electron transfer in photosynthetic reaction centers, *J. Bioenerg. Biomembr. 27*, 275−283.
19. Narváez, A. J., Kálmán, L., LoBrutto, R., Allen, J. P., and Williams, J. C. (2002) Influence of the protein environment on the properties of a tyrosyl radical in reaction centers from *Rhodobacter sphaeroides*, *Biochemistry 41*, 15253−15258.
20. Kálmán, L., Williams, J. C., and Allen, J. P. (2003) Proton release upon oxidation of tyrosine in reaction centers from *Rhodobacter sphaeroides*, *FEBS Lett. 545*, 193−198.
21. Williams, J. C., Alden, R. G., Murchison, H. A, Peloquin, J. M., Woodbury, N. W., and Allen, J. P. (1992) Effects of mutations near the bacteriochlorophylls in reaction centers from *Rhodobacter sphaeroides*, *Biochemistry 31*, 11029−11037.
22. Kleinherenbrink, F. A. M., Chiou, H. C., LoBrutto, R., and Blankenship, R. E. (1994) Spectroscopic evidence for the presence of an iron−sulfur center similar to F-X in photosystem I in *Heliobacillus mobilis*, *Photosynth. Res. 41*, 115−123.
23. Narváez, A. J., LoBrutto, R., Allen, J. P., and Williams, J. C. (2004) Trapped tyrosyl radical populations in modified reaction centers from *Rhodobacter sphaeroides*, *Biochemistry*, in press.
24. Kálmán, L., LoBrutto, R., Narváez, A. J., Williams, J. C., and Allen, J. P. (2003) Correlation of proton release and electrochromic shifts of the optical spectrum due to oxidation of tyrosine in reaction centers from *Rhodobacter sphaeroides*, *Biochemistry 42*, 13280−13286.
25. Graige, M. S., Paddock, M. L., Bruce, J. M., Feher, G., and Okamura, M. Y. (1996) Mechanism of proton-coupled electron transfer for quinone (Q_B) in reaction centers of *Rb. sphaeroides*, *J. Am. Chem. Soc. 118*, 9005−9016.
26. Diner, B. A., Force, D. A., Randall, D. W., and Britt, R. D. (1998) Hydrogen bonding, solvent exchange, and coupled proton and electron transfer in the oxidation and reduction of redox-active tyrosine Y_Z in Mn-depleted core complexes of photosystem II, *Biochemistry 37*, 17931−17943.

27. Tommos, C., Skalicky, J. J., Pilloud, D. L., Wand, A. J., and Dutton, P. L. (1999) *De novo* proteins as models of radical enzymes, *Biochemistry 38*, 9495−9507.
28. Faller, P., Goussias, C., Rutherford, A. W., and Un, S. (2003) Resolving intermediates in biological proton-coupled electron transfer. A tyrosyl radical prior to proton movement, *Proc. Natl. Acad. Sci. U.S.A. 100*, 8732−8735.
29. Diner, B. A., and Babcock, G. T. (1996) Structure, dynamics, and energy conversion efficiency in photosystem II in *Oxygenic Photosynthesis: The Light Reactions* (Ort, D., and Yocum, C., Eds.) pp 213−247, Kluwer Academic Publishers, Dordrecht, The Netherlands.
30. Hammarström, L., Sun, L., Åkemark, B., and Styring, S. (2001) A biomimetic approach to artificial photosynthesis: Ru(II)-polypyridine photo-sensitisers linked to tyrosine and manganese electron donors, *Spectrochim. Acta, Part A 37*, 2145−2160.
31. Ahlbrink, R., Haumann, M., Cherepanov, D., Bögershausen, O., Mulkidjanian, A., and Junge, W. (1998) Function of tyrosine Z in water oxidation by photosystem II: Electrostatical promotor instead of hydrogen abstractor, *Biochemistry 37*, 1131−1142.

BI0362727